Electronic Supplementary Material (ESI) for RSC Advances


# Supporting Information for Chrysanolide A, an unprecedented sesquiterpenoid trimer from the Flowers of *Chrysanthemum indicum* L.

Qiong Gu,*[a] Yaoyao Chen,[b] Hui Cui,[a] Dane Huang,[a] Jing-wei Zhou,[a] Taizong Wu,[a] Yiping Chen,[b] Lina Shi [a] and Jun Xu *[a]

[a] *Research Center for Drug Discovery & Institute of Human Virology, School of Pharmaceutical Sciences, Sun Yat-Sen University, Guangzhou 510006, P.R. China.*

[b] *Guangxi University of Chinese Medicine, Guangxi 530001, P.R. China*

**Contents of Supporting Information**

## Detailed experimental procedures

**General Experimental Procedures.** 1D and 2D NMR spectra were recorded on a Bruker AM-400 NMR spectrometer with TMS as the internal standard (Bruker, Bremerhaven, Germany). IR (KBr) spectra were recorded on a Bio-Rad FTS-135 spectrometer (Bio-Rad, Hercules, CA, USA). UV data were collected on a Shimadzu UV-2401A spectrophotometer (Shimadzu, Kyoto, Japan). Optical rotations were collected on a Jasco model 1020 polarimeter (Horiba, Tokyo, Japan). Silica gel (200-300 mesh and H) for column chromatography was obtained from Qingdao Meigao Chemical Company (Makall, Qingdao, China). Sephadex LH-20 (20-150 μm) was purchased from Pharmacia Fine Chemicals Co. Ltd. (Pharmacia, Uppsala, Sweden). The analytical and preparation HPLC was performed with a LC-20A system equipped with Agilent SB-18 column (4.6*250 mm, 5 μm) or Agilent SB-18 column (9.6*250 mm, 5 μm).

**Computational Methods**. The theoretical $^{1}$H NMR and CD spectra, and transition state were performed by density functional theory (DFT) and time-dependent DFT (TD-DFT), respectively, using Gaussian 09 and analyzed using GUIs GaussView (version 5.0). The theoretical $^{1}$H NMR spectra calculations were first performed at HF/6-31G level in the gas phase for initial optimization. The corresponding minimum geometries were fully optimized at the B3LYP/6-31G (d) level in gas phase to get more accurate conformers. The $^{1}$H NMR shielding constants were computed using the GIAO technique at the B3LYP/6-31+G(d,p) level for C, H and B3LYP/6-31+G(2d,p) level for O in the PCM solvent continuum model with chloroform as a solvent. The $^{1}$H NMR chemical shifts were calculated as $\delta = \sigma_{ref} - \sigma$, where $\sigma_{ref}$ was the shielding constant of TMS calculated at the same level of theory (192.9341ppm). The ECD spectra were simulated at B3LYP/6-31G (d, p) leve in MeOH. The calculated ECD curve was generated using SpecDis with σ=0.2Ev. The transition state calculations were performed at the M062X/6-31G(d) level of theory in the gas phase to obtain the transition state. Then the obtained transition states, their reactants and products were fully optimized at M062X/6-31G(d) level of theory in three systems (in gas phase, eps=4 with unspecified solution and chorlform).

**Extraction and Isolation.**

Flowers of *C. indicum* L. were collected from Hubei, China. The identity of the plant material was verified by one of the authors (Qing Gu), and a voucher specimen (SYSU20100801) has been deposited in Research Center for Drug Discovery, School of Pharmaceutical Sciences, Sun Yat-Sen University, Guangzhou, People's Republic of China.

The air-dried and powdered flowers of *C. indicum* L. (5.1 kg) were extracted with 95% EtOH for three days at room temperature (three times), and the combined extracts were concentrated in vacuo (under 50℃). The resulting dark extracts were suspended in $H_2O$ and extracted sequentially with petrol ether, EtOAc, and n-BuOH (saturated with $H_2O$). The EtOAc-soluble extract 300 g was subjected to CC on silica gel using petrol ether, $CHCl_3$, $Me_2CO$, and MeOH for elution to give four fractions. The combined $CHCl_3$ fraction (100 g), eluted with petrol ether-EtOAc mixtures of increasing polarity, was chromatographed over silica gel to afford 7 fractions (Fr. A-G). Fr. A (20 g) was fractioned over Sephadex LH-20 ($CHCl_3$-MeOH, 1:1), purified with preparation HPLC to give compounds **1** (10 mg) and **2** (25 mg). Fr. D (15.3 g) were chromatographed over silica gel (200-300 mesh), eluted in a step gradient manner with petrol ether-EtOAc (8:2 to 5:5) to afford six subfractions. Subfractions D-1 (2.5 g) was fractionated over Sephadex LH-20 ($CHCl_3$-MeOH, 1:1) to yield a mixture (400 mg) that was subjected to Rp-18 CC eluting with 60% MeOH in $H_2O$ and 80%. Three fractions were obtained, of which fraction 2 (100 mg) was submitted to preparation HPLC to give two compound **3** (15 mg).

**Chrysanolide A (3)**: colorless powder; $[\alpha]_D^{15}$ -78.74 (c 0.13, $CHCl_3$); UV ($CHCl_3$) $\lambda max$ (log ε) 209 (3.26) nm; IR (KBr) $\nu_{max}$ 3504, 2963, 2933, 1750, 1456, 1373, 1264, 1142, 1030, 992, 672 $cm^{-1}$; $^1H$ and $^{13}C$ NMR data, see Table 1; EIMS *m/z* 474, 306, 288, 264, 246, 228; positive HRESIMS *m/z* 821.3969 $[M+Na]^+$ (calcd for $C_{47}H_{58}O_{11}Na$).

**Anti-HBV Activity Assay.**

The anti-HBV procedure was performed according to our previous report. The HepG 2.2.15 cell, which was stably transfected with the HBV genome, was used in this study. Compounds stock solutions were prepared in DMSO and stored at -20℃. Upon dilution with DMEM culture medium, the final DMSO concentration was ≤ 0.5%, a concentration having no effect on cell replication. Cells were maintained in DMEM (Gibco) supplemented with 100 μg/mL penicillin, 100 μg/ mL streptomycin, 500 μg/ mL G418, and 10% fetal bovine serum (Gibco) at 37℃ in an incubator with 5% $CO_2$. The HepG 2.2.15 cell suspensions were seeded in 24-well microtiter plates and cultured for 48 h. Then, they were incubated at 37° C for 6 days in the presence of test compounds (200, 100, 50, and 25 μM) from the DMSO-diluted stock solution. The medium was refreshed every 3 days. Then, the culture supernatants were harvested to detect the HBsAg and HBeAg secretions using appropriate diagnostic ELISA kits (Shanghai SIIC KEHUA Biotech Co. Ltd.) as described in triplicate, and the SEM (standard error of the mean) of inhibition values varied no more than 5%. The samples were diluted to appropriate concentrations with PBS buffer before measurement. Inhibition rates (percent) of antigens were calculated as [1－

value of the study well (A450-A630)/value of the control well with drug (A450-A630)] *100%. The concentration of the chemicals with an inhibition rate 50% ($EC_{50}$) were calculated according to Berkson's method. Cell damage was assessed by means of the MTT assay.

**Fig. S1** Selected NOESY correlations (double arrows) of compound **1**

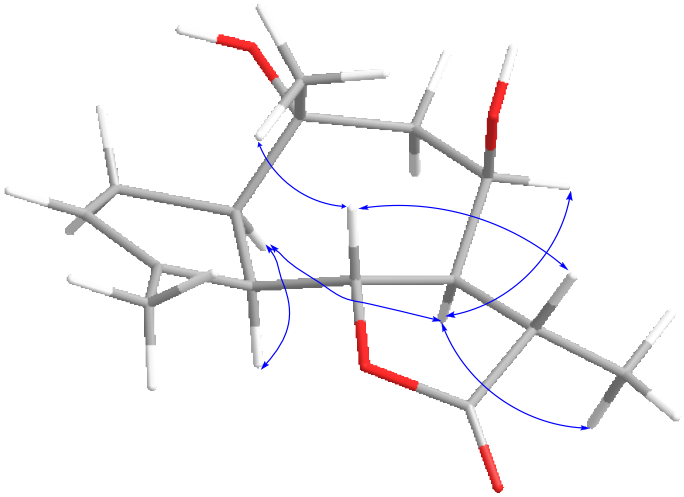

**Fig. S2** Key HMBC (arrows) and NOESY (double arrows) correlations of compound **2**

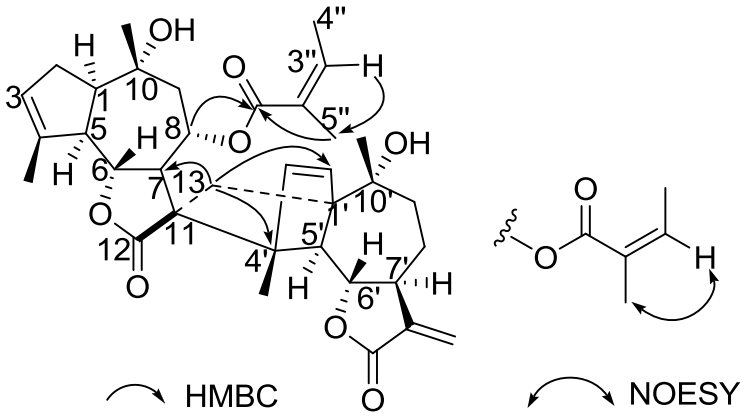

**Fig. S3** UV spectrum of compound **3**

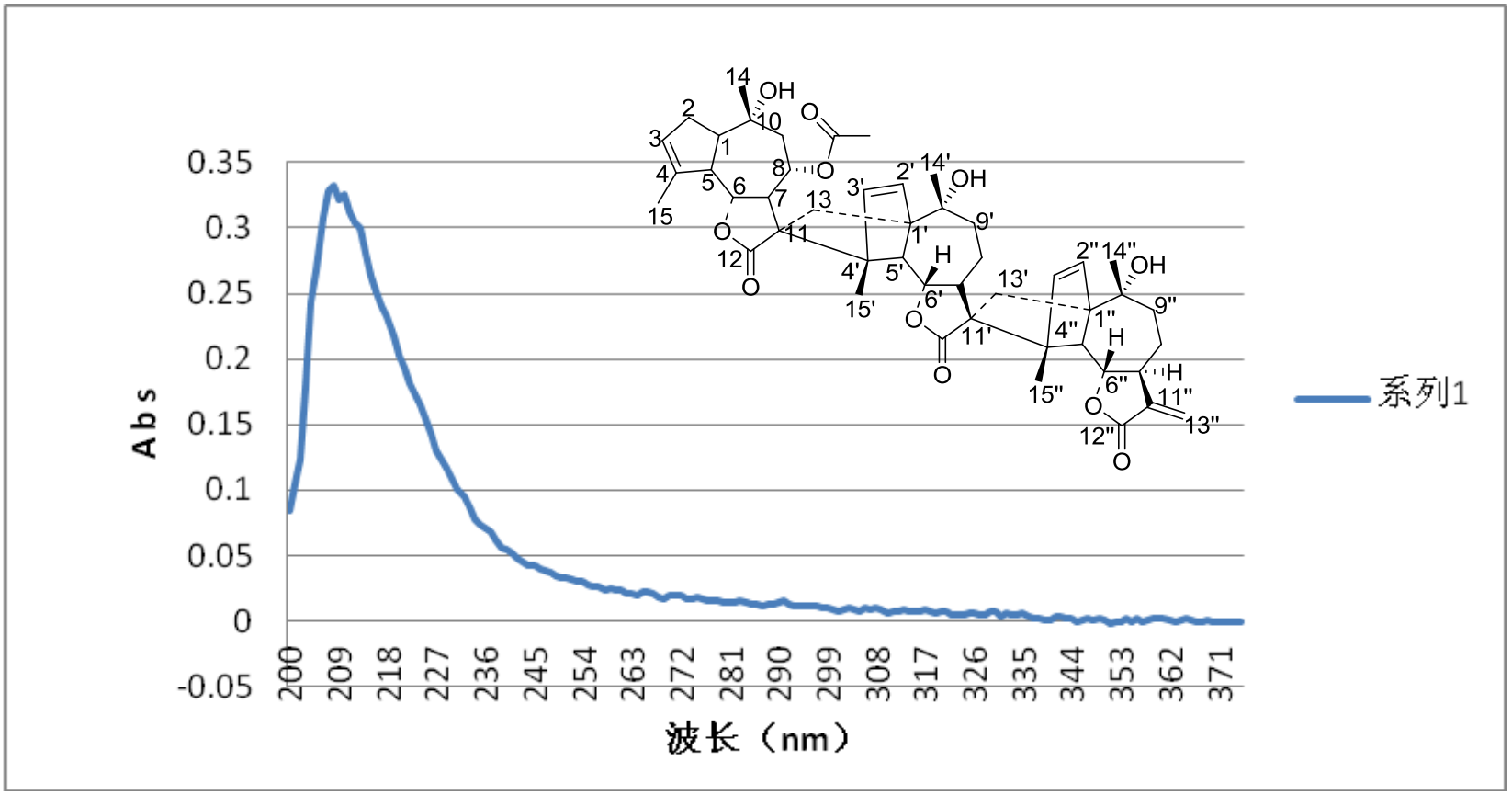

# **Fig. S4** IR spectrum of compound **3**

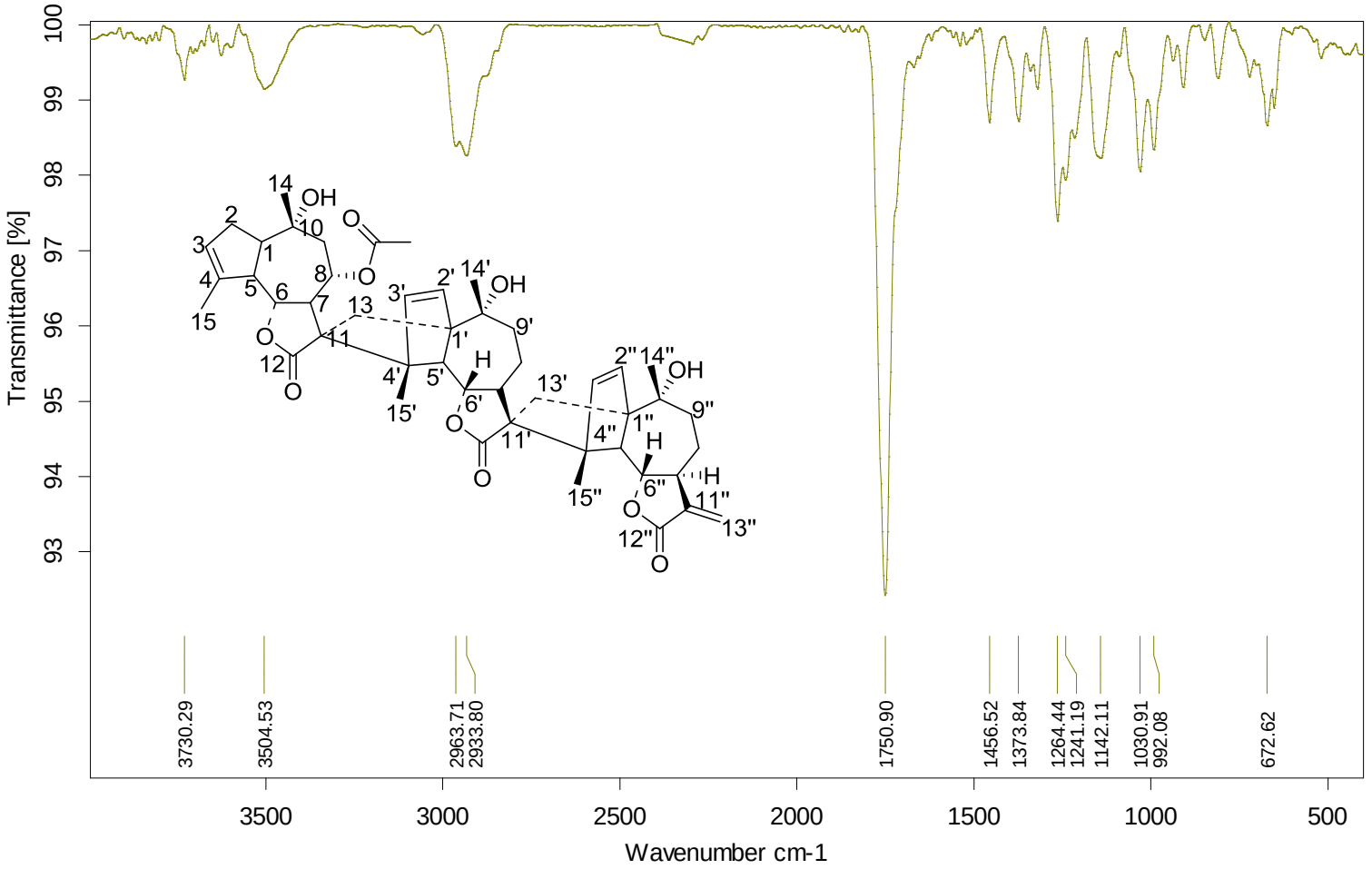


| | | | |
|---|---|---|---|
| D:\CUIHUI\CI-26-bg.0 | CI-26-bg | solid | 08/09/2012 |

# **Fig. S5** $^1$H NMR spectrum of compound **3** in $CDCl_3$

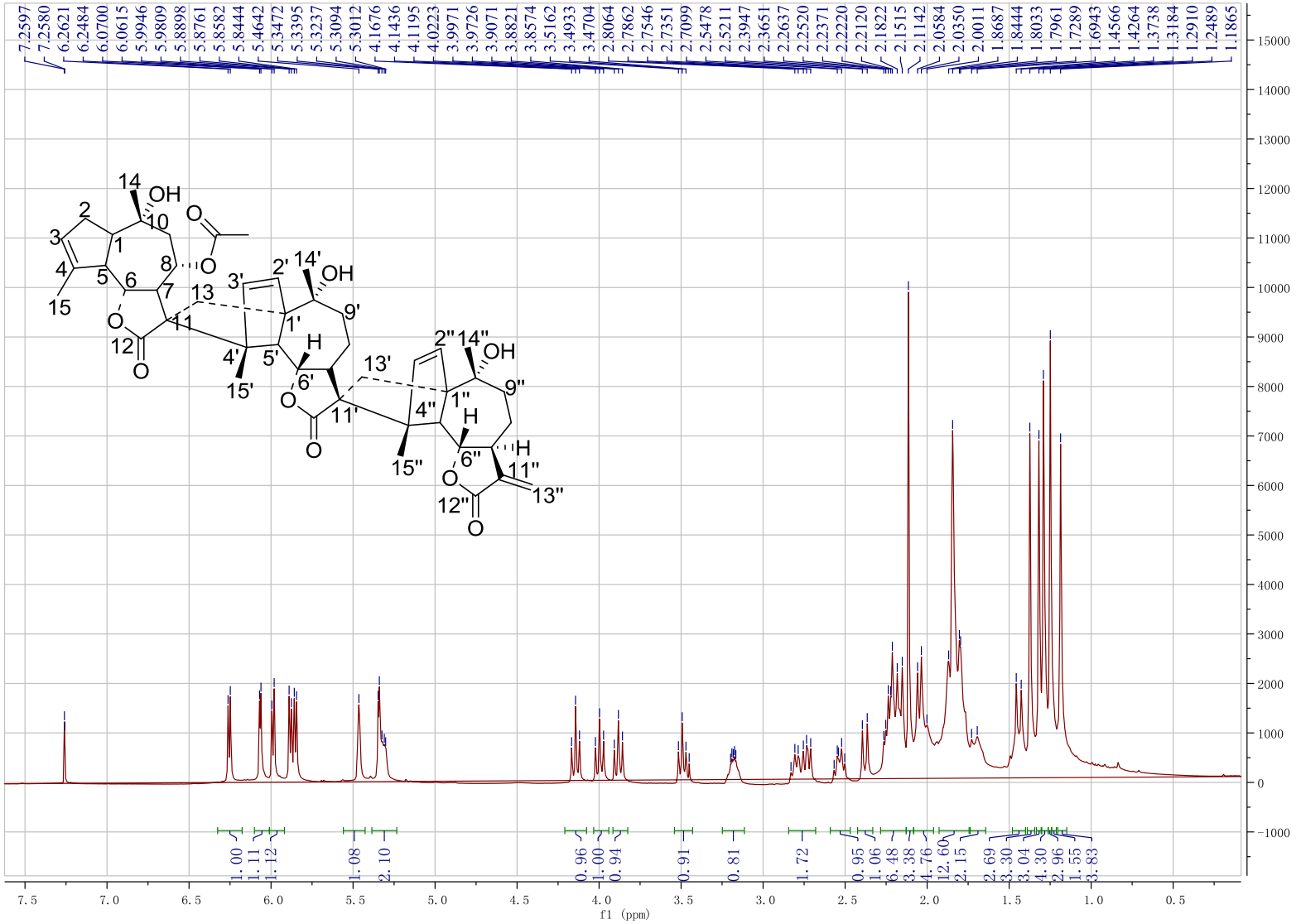

**Fig. S6** $^{13}C$ NMR spectrum of compound **3** in $CDCl_3$

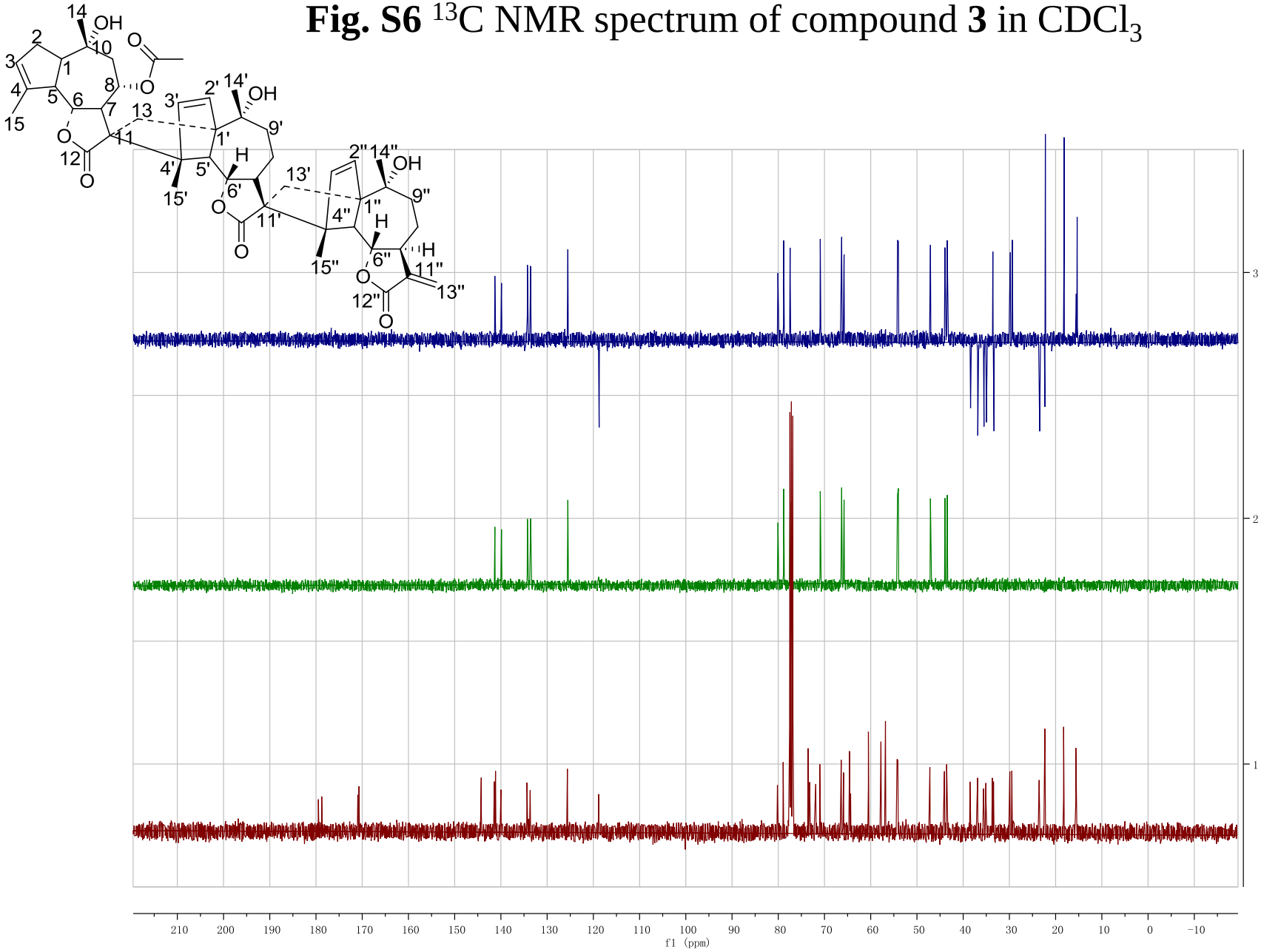

Electronic Supplementary Material (ESI) for RSC Advances


# **Fig. S7** $^{1}$H-$^{1}$H COSY NMR spectrum of compound **3** in $CDCl_3$

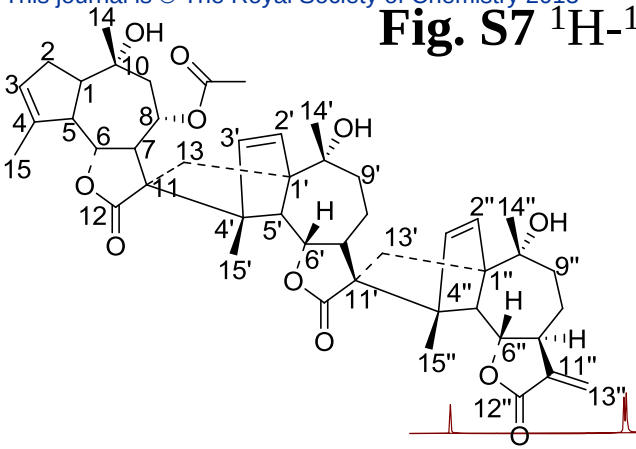


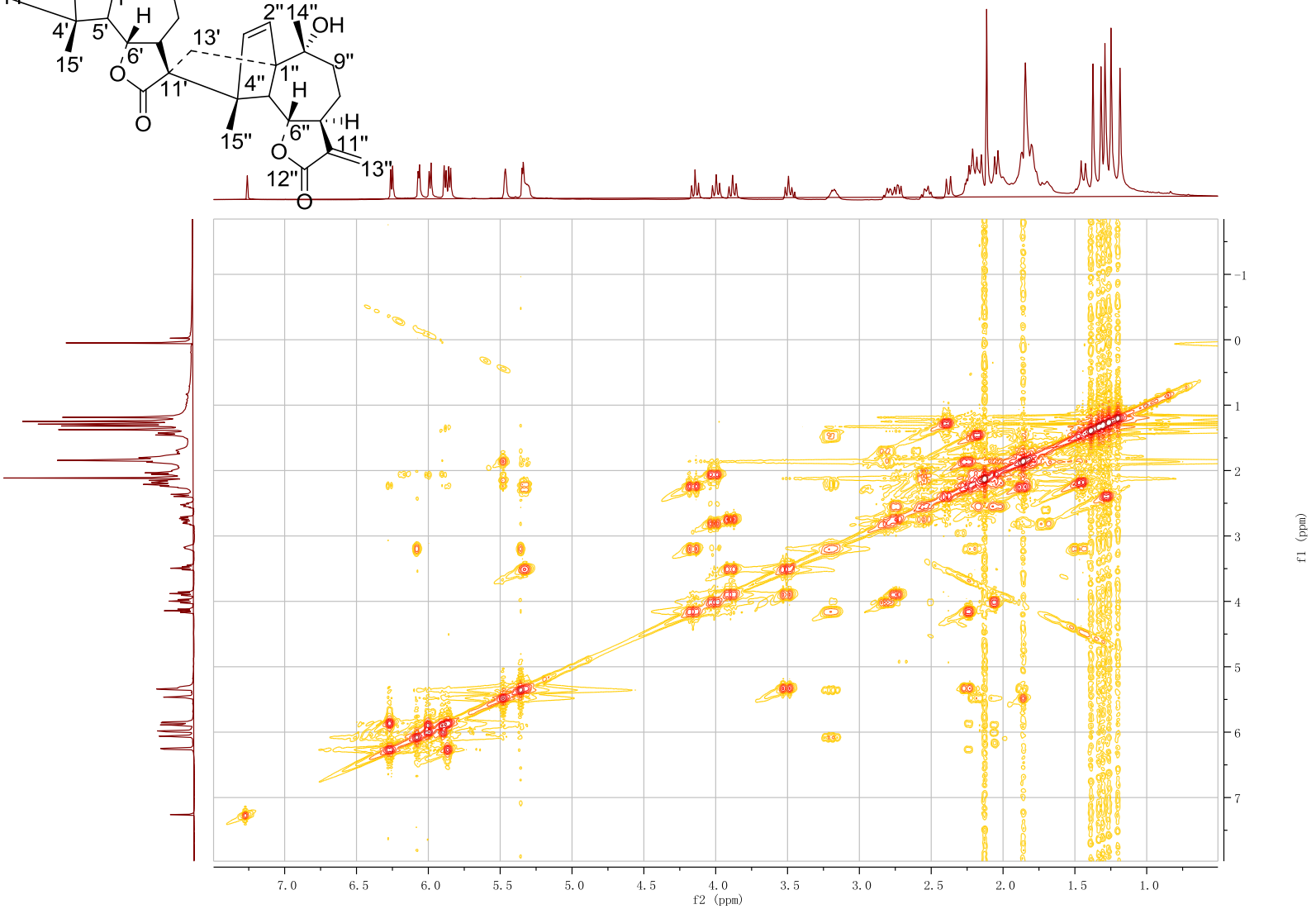

**Fig. S8** HSQC NMR spectrum of compound **3** in $CDCl_3$

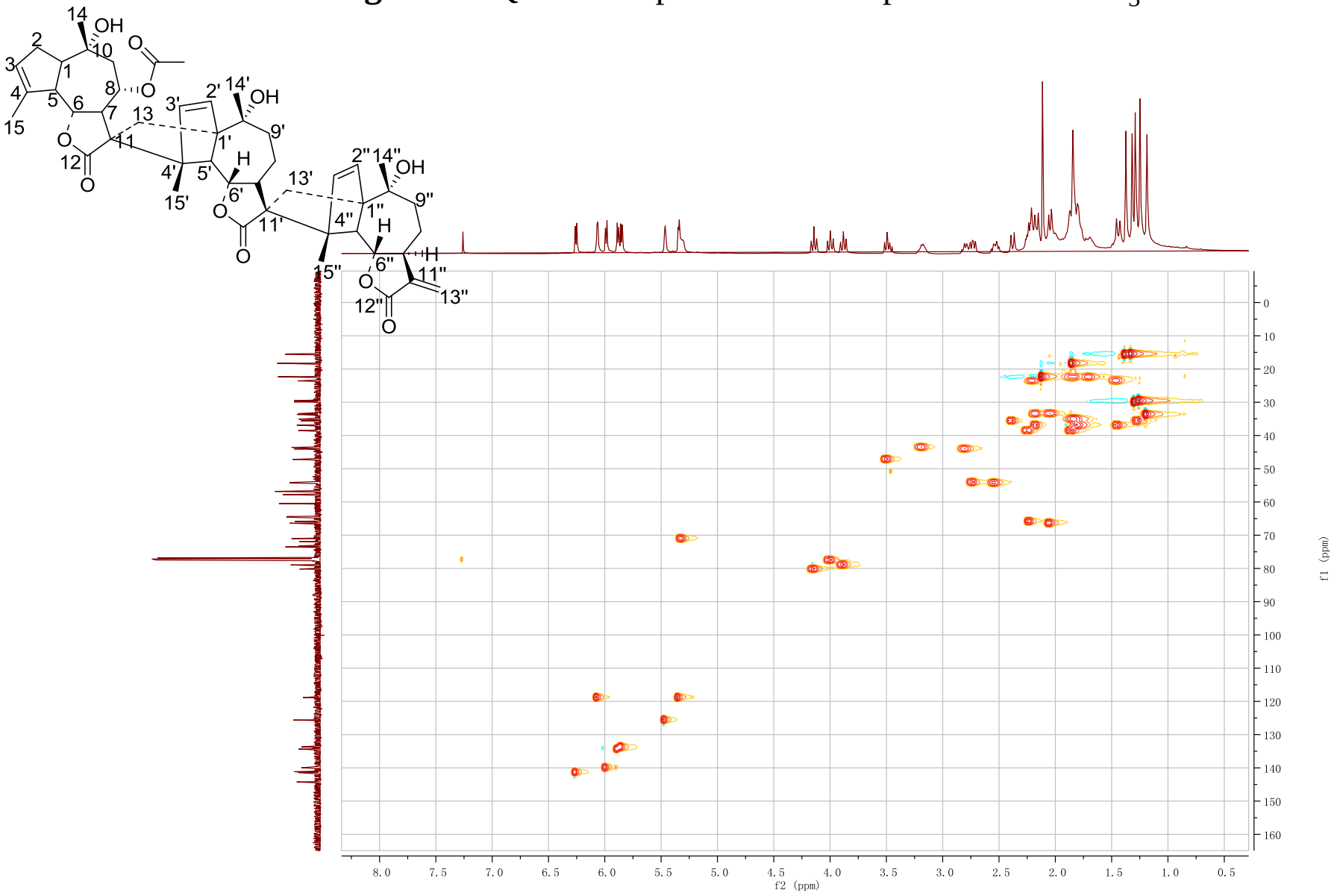

# Fig. S9 HMBC NMR spectrum of compound **3** in $CDCl_3$

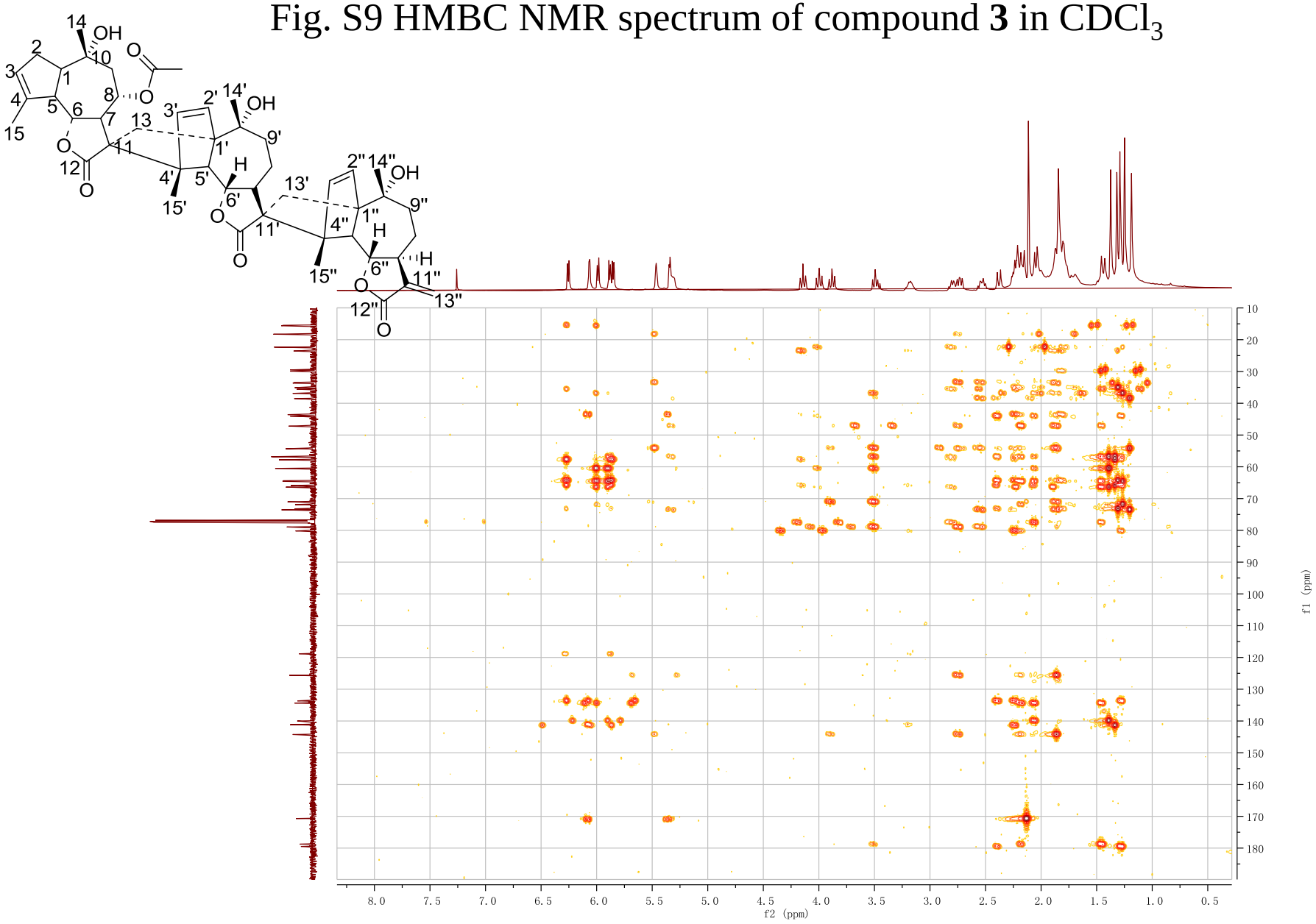

# **Fig. S10** ROESY NMR spectrum of compound **3** in $CDCl_3$

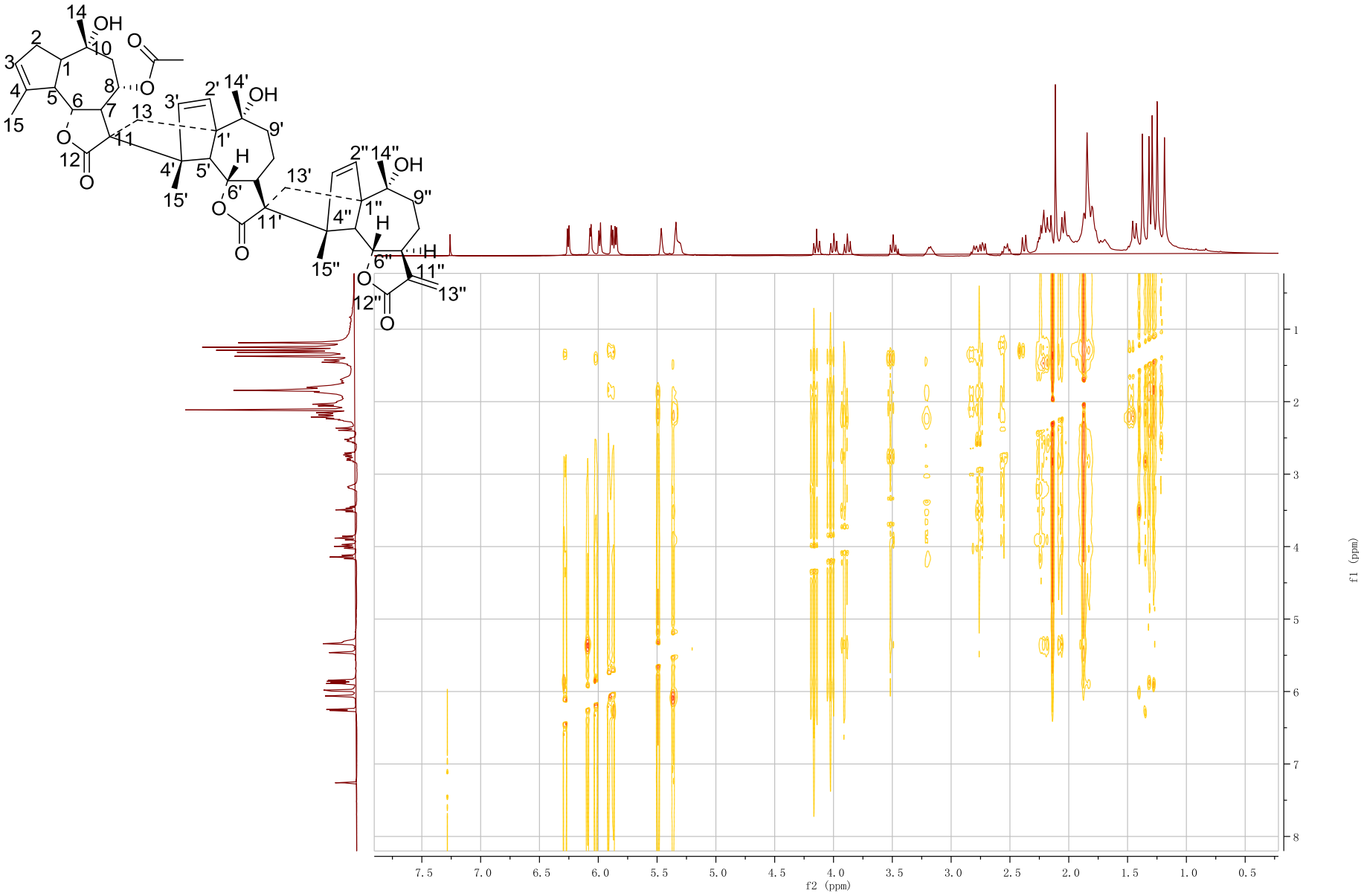

# **Fig. S11** EI spectrum of compound **3**

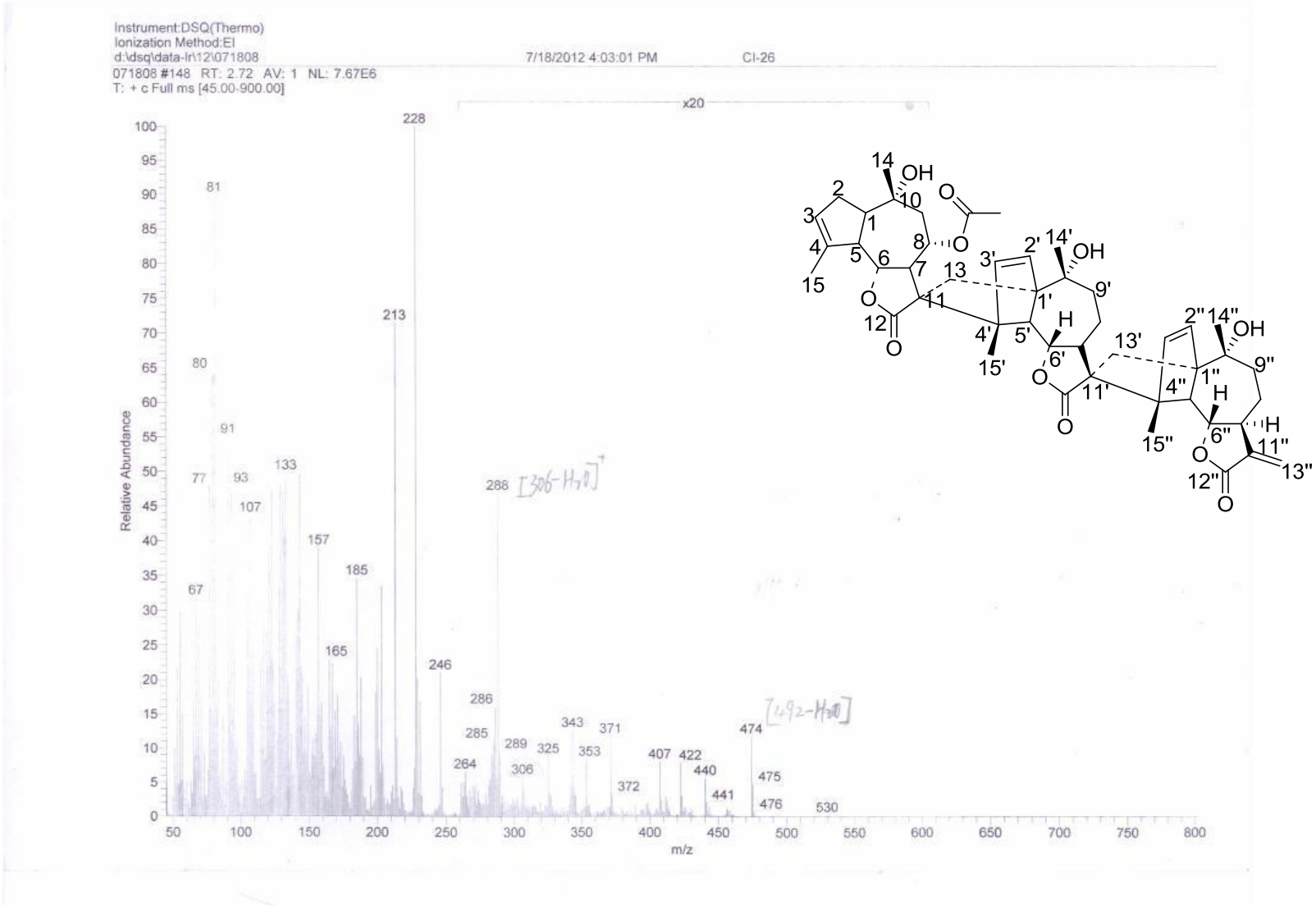

# **Fig. S12** HRESIMS spectrum of compound **3**

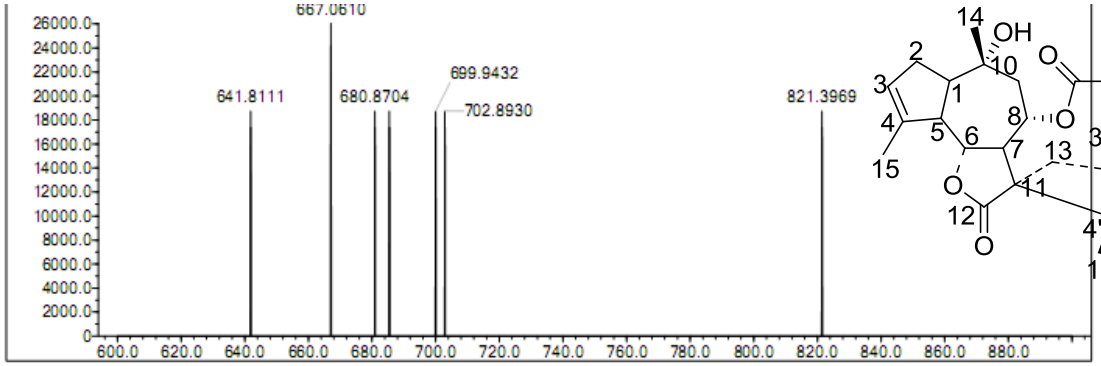


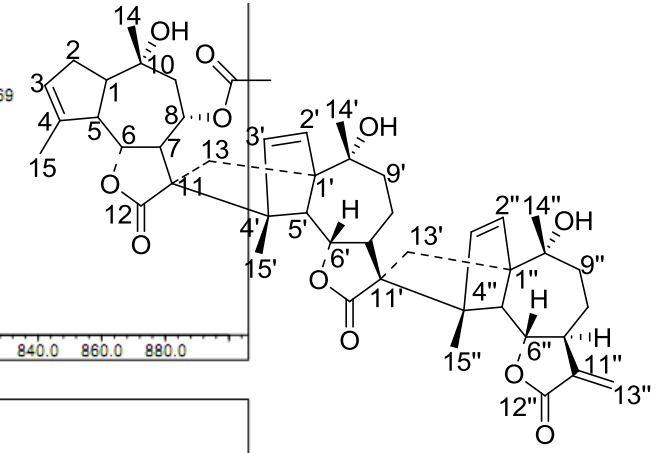


Measured region for 821.3969 m/z

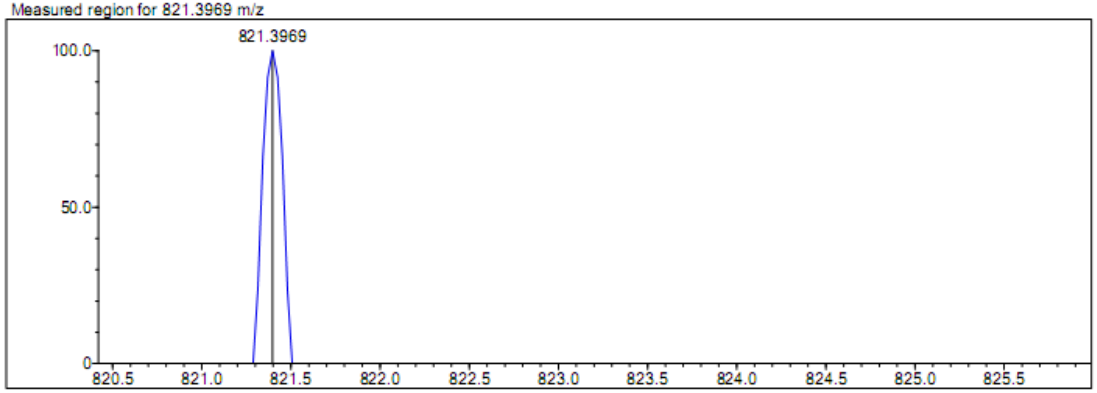


C47 H58 O11 [M+Na]+ : Predicted region for 821.3871 m/z

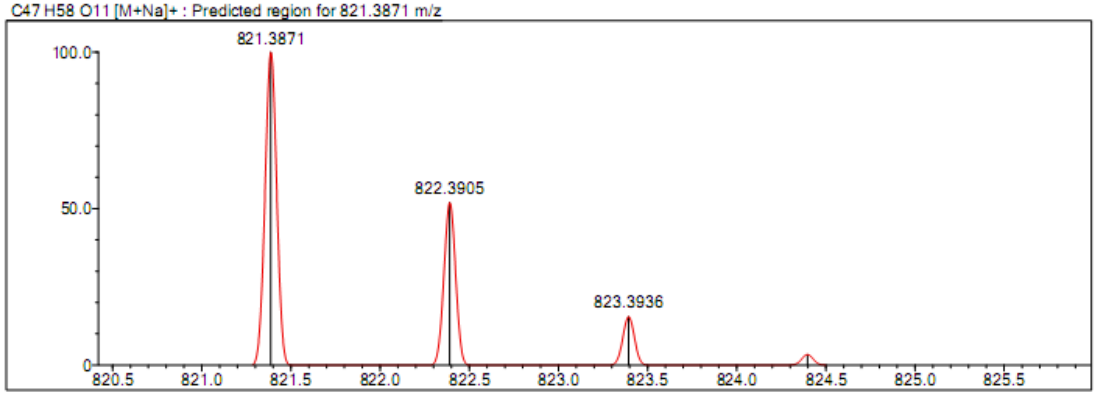


| Rank | Score | Formula (M) | Ion | Meas. m/z | Pred. m/z | Df. (mDa) | Df. (ppm) | Iso | DBE |
|---|---|---|---|---|---|---|---|---|---|
| 3 | 0.00 | C47 H58 O11 | [M+Na]+ | 821.3969 | 821.3871 | 9.8 | 11.93 | 0.00 | 19.0 |

# Fig. S13 $^{1}$H NMR spectrum of compound **1** in $CDCl_3$

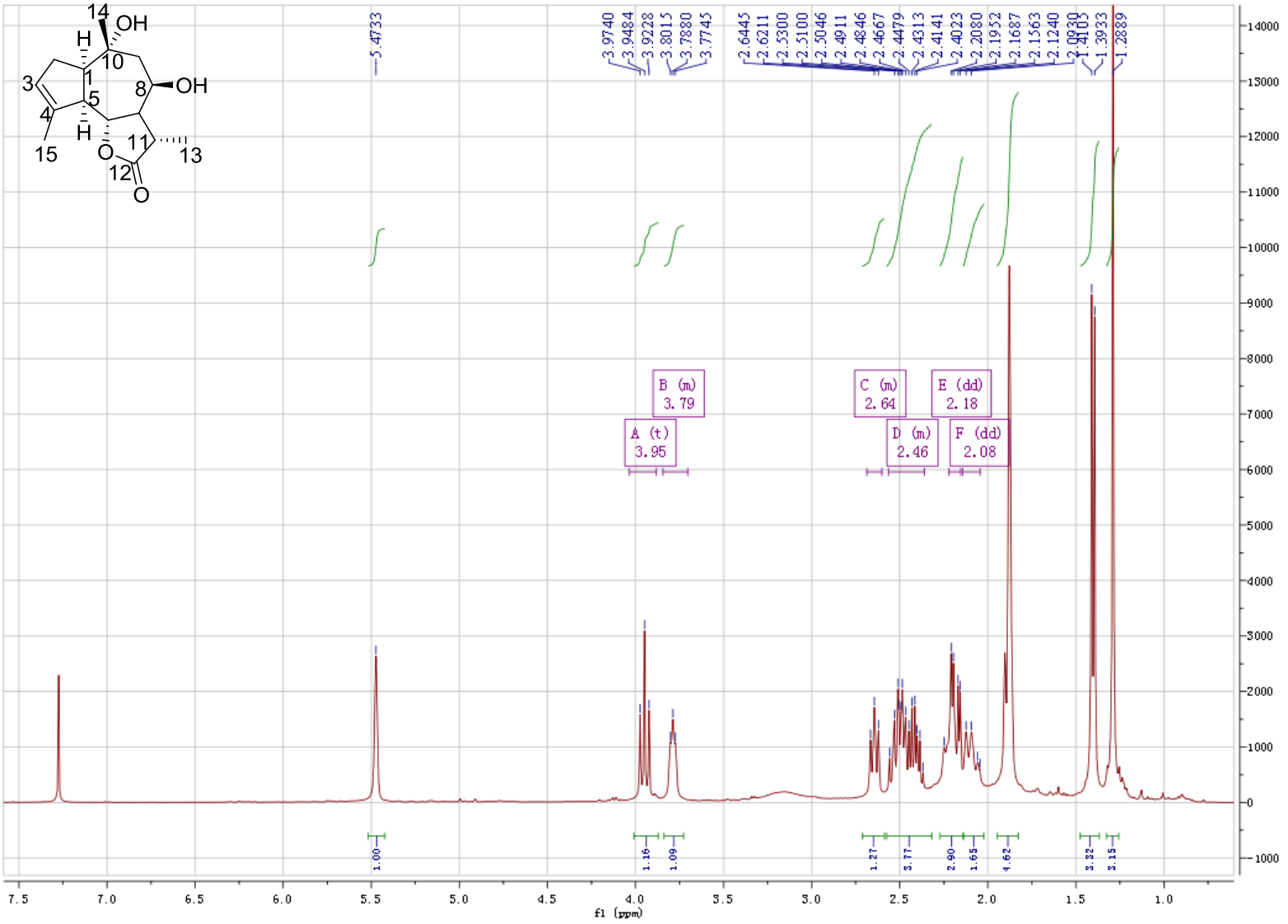

# **Fig. S14** $^{13}$C NMR spectrum of compound **1** in $CDCl_3$

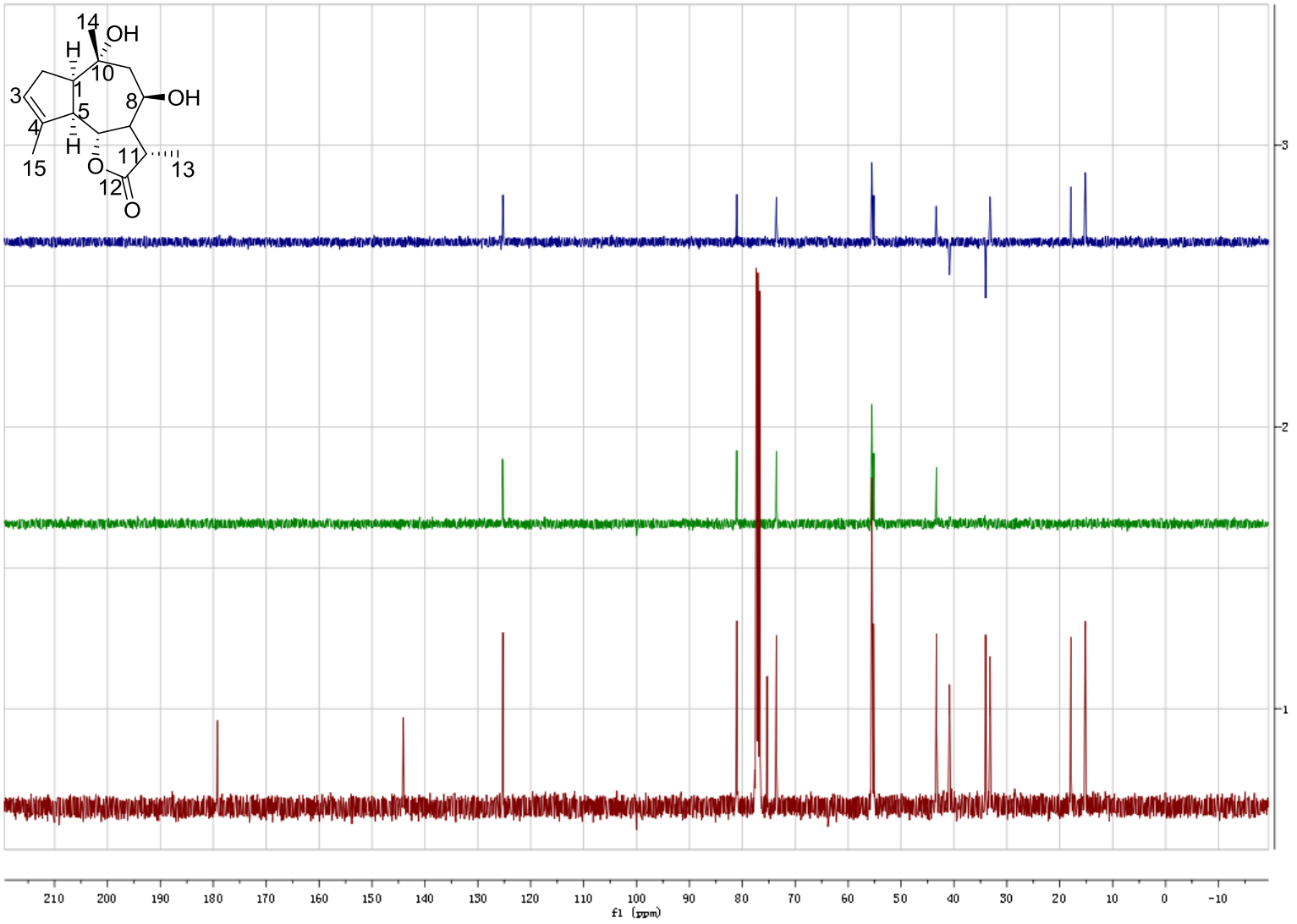

# **Fig. S15** $^{1}$H NMR spectrum of compound **2** in $CDCl_3$

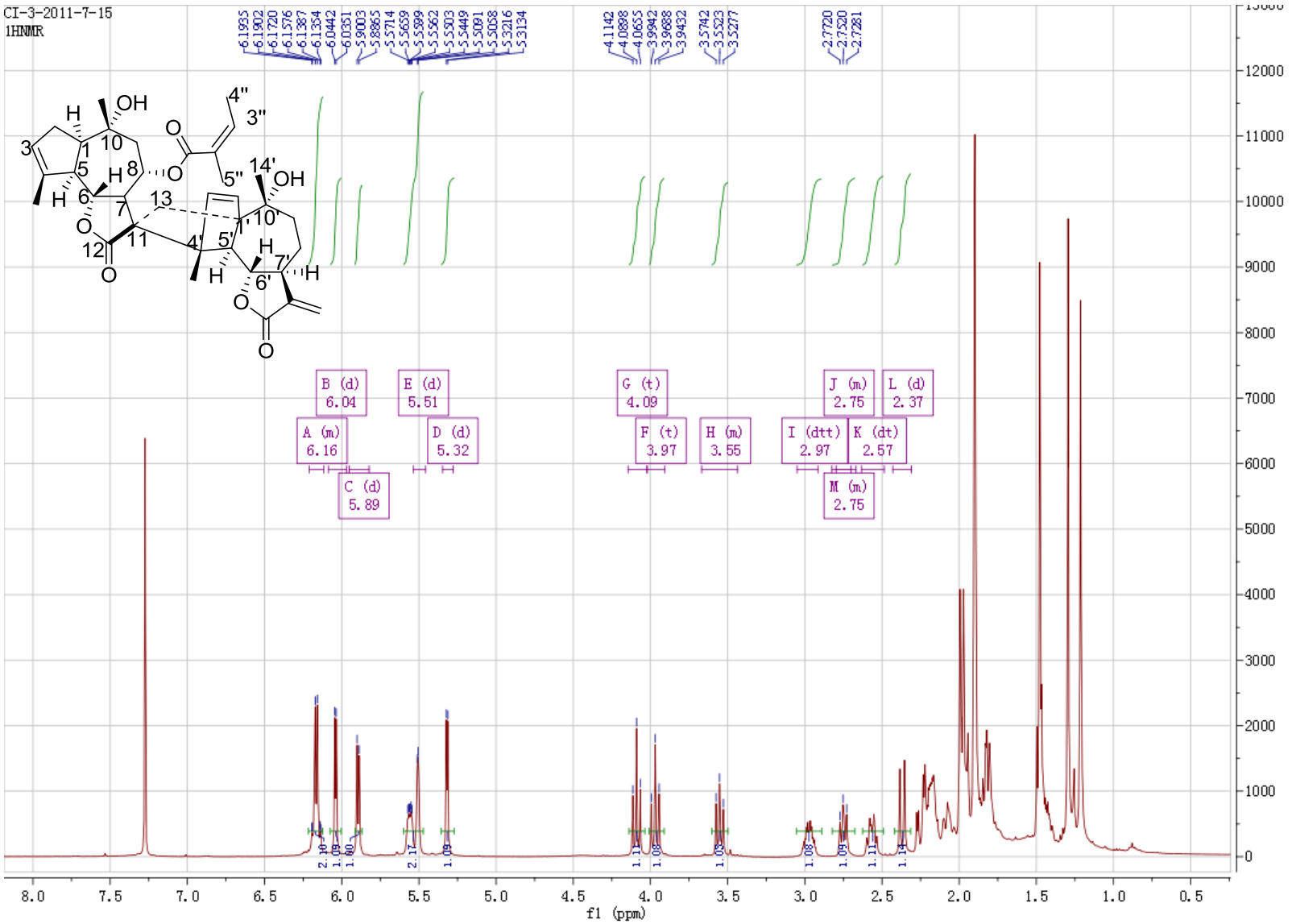

# **Fig. S16** $^{13}$C NMR spectrum of compound **2** in $CDCl_3$

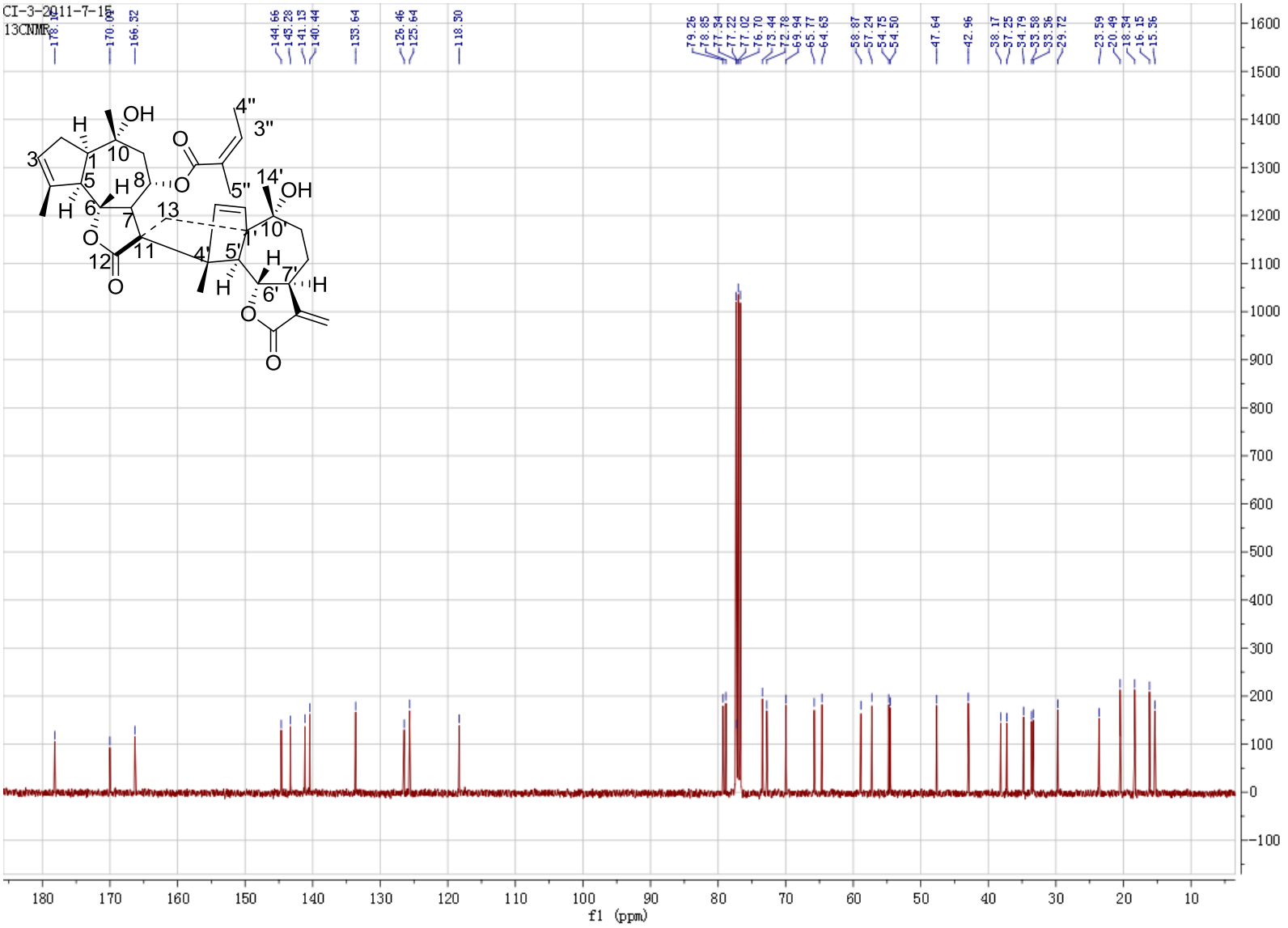

**Fig. S17** The geometries of compound **3**

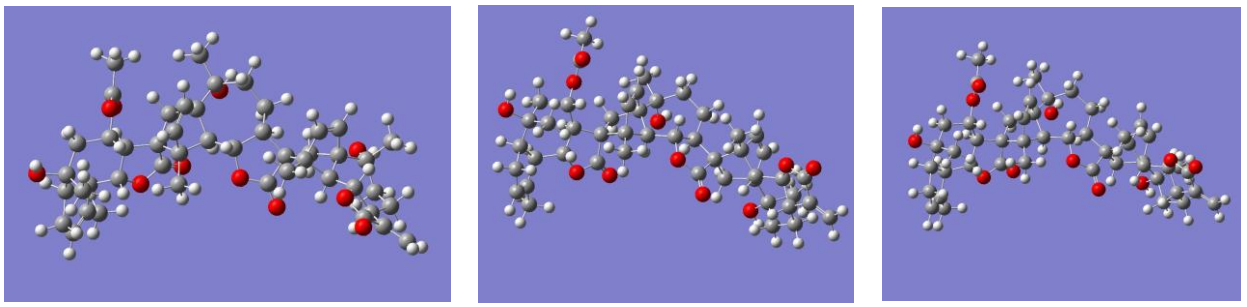

Unoptimized geometries

Optimized geometries at the B3LYP/6-31+G (d,p) level in the gas phase

Optimized geometries at the B3LYP/6-31+G (d,p) level in the chloroform solutions

**Fig. S18** Comparison of experimental vs. calculated $^{1}$H NMR chemical shifts of compound **3** (ppm)

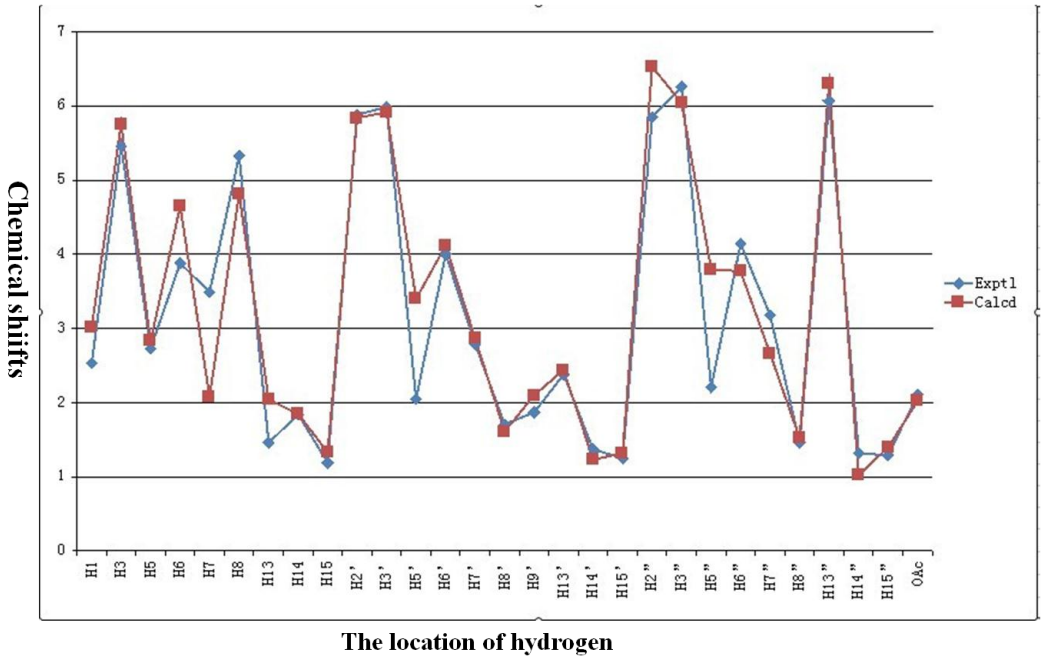

**Fig. S19** Transition state from monomer to trimer at M062X/6-31+G(d) level in the gas phase

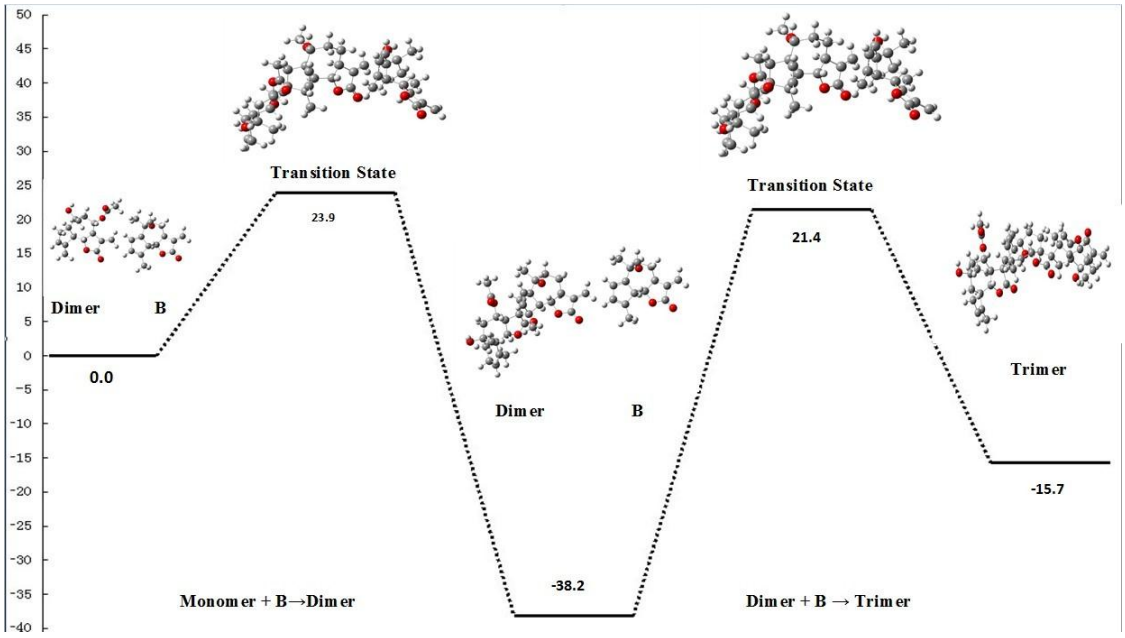


**Fig. S20** Transition state from monomer to trimer at M062X/6-31+G(d) level of PCM solvent continuum model with chloroform as a solvent

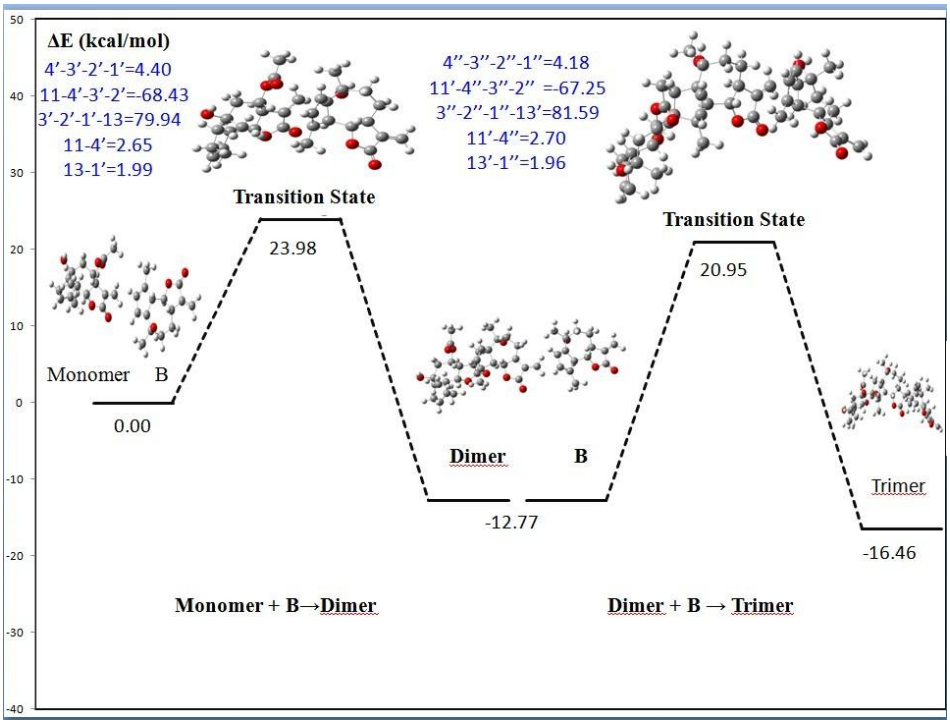

**Fig. S21** Transition state from monomer to trimer at M062X/6-31+G(d) level of PCM solvent continuum model with unspecified solvent

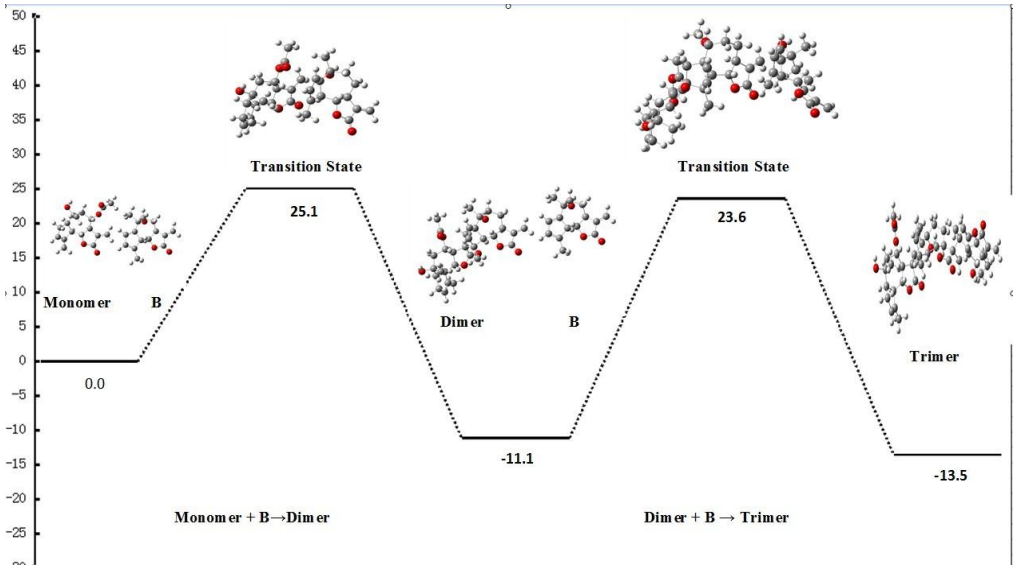

**Table S1** Experimental and calculated NMR data for **1** in $CDCl_3$ ($\delta$ in ppm, $J$ in Hz)

| $^1$H NMR | | | | $^{13}$C NMR |
|---|---|---|---|---|
| No. | *Exptl*[a] | *Calcd* | $\Delta\ \delta$[c] | *Exptl*[b] |
| **1** | 2.49 (1H, dd, 16.7, 8.1) | 2.54 | 0.05 | 55.5 d |
| **2** | 2.22 (1H, m); | 2.28 | 0.06 | 34.1 t |
| | 2.09 (1H, m, overlap) | 2.19 | 0.1 | |
| **3** | 5.47 (1H,br.s) | 5.76 | 0.29 | 125.3 d |
| **4** | | | | 144.0 s |
| **5** | 2.66 (1H, t, 8.9) | 2.56 | 0.1 | 55.3 d |
| **6** | 4.04 (1H, t, 10.4) | 4.07 | 0.03 | 81.7 d |
| **7** | 3.02 (1H, dd, 18.7, 9.5) | 2.94 | 0.08 | 50.4 d |
| **8** | 3.94 (1H, t like) | 3.96 | 0.02 | 66.7 d |
| **9** | 2.09 (1H, m, overlap); | 2.12 | 0.03 | 40.6 t |
| | 1.94 (1H, d, 15.6) | 1.62 | 0.32 | |
| **10** | | | | 75.1 s |
| **11** | 2.90 (1H, dd, 15.3, 7.7) | 3.03 | 0.13 | 37.4 d |
| **12** | | | | 180.2 s |
| **13** | 1.25 (1H, d, 7.6) | 1.19 | 0.06 | 12.1 q |
| **14** | 1.29 (s) | 1.11 | 0.18 | 32.9 q |
| **15** | 1.88 (s) | 1.95 | 0.07 | 17.8 q |

Largest deviation [c]$\Delta\delta$ = 0.32 ppm. [a]In 400. [b]In 100 MHz. [c]$\boldsymbol{\Delta\delta}$ = |$\delta$calcd - exptl|.

**Table S2** Experimental and calculated NMR data for **2** in $CDCl_3$ ($\delta$ in ppm, $J$ in Hz)

| $^1$H NMR of **2** | | | | $^{13}$CNMR of **2** |
|---|---|---|---|---|
| No | Exptl[a] | Calcd | $\Delta\delta$[c] | Exptl[b] |
| 1 | 2.57 (1H, dt, 15.3, 7.6) | 2.85 | 0.28 | 54.5 d |
| 2 | 2.24-2.04 (2H, m) | 2.79 | 0.55 | 33.6 t |
| 3 | 5.49 (1H, br. s) | 5.94 | 0.45 | 125.6 d |
| 4 | | | | 144.7 s |
| 5 | 2.75 (1H, t, 8.0) | 2.40 | 0.35 | 54.8 d |
| 6 | 3.96 (1H, t, 8.0) | 4.57 | 0.61 | 78.8 d |
| 7 | 3.54 (1H, t, 8.0) | 2.35 | 1.19 | 47.6 d |
| 8 | 5.56 (1H, m) | 5.29 | 0.27 | 69.9 d |
| 9 | 2.26 (1H, 4.5) | 1.86 | 0.4 | 38.2 t |
| | 2.21 (1H, 4.5) | 1.67 | 0.54 | |
| 10 | | | | 73.4 s |
| 11 | | | | 58.9 s |
| 12 | | | | 178.2 s |
| 13 | 2.37 (2H, d, 12.1) | 2.40 | 0.03 | 37.2 t |
| 14 | 1.21 (3H, s) | 1.49 | 0.28 | 33.4 q |
| 15 | 1.89 (3H, s) | 1.85 | 0.04 | 18.3 q |
| 1’ | | | | 65.8 s |
| 2’ | 5.88 (1H, d, 5.5) | 6.06 | 0.18 | 133.6 d |
| 3’ | 6.18 (1H, d, 5.5) | 6.35 | 0.17 | 140.4 d |
| 4’ | | | | 57.2 s |
| 5’ | 1.95 (1H, m) | 3.46 | 1.51 | 64.6 d |
| 6’ | 4.08 (1H, t, 9.7) | 4.00 | 0.08 | 79.3 d |
| 7’ | 2.95 (1H, m) | 3.58 | 0.63 | 43.0 d |
| 8’ | 2.18 (1H, m) | 2.05 | 0.13 | 23.6 t |
| | 1.46 (1H, m) | 1.39 | 0.07 | |
| 9’ | 1.80 (m) | 1.71 | 0.09 | 34.8 t |
| 10’ | | | | 72.8 s |
| 11’ | | | | 141.3 s |
| 12’ | | | | 170.0 s |
| 13’ | 6.02 (1H, d, 3.6) | 6.29 | 0.27 | 118.3 t |
| | 5.31 (1H, d, 3.6) | 5.57 | 0.26 | |
| 14’ | 1.46 s | 1.57 | 0.11 | 15.4 q |
| 15’ | 1.28 s | 1.13 | 0.15 | 29.7 q |
| 1” | | | | 166.3 s |
| 2” | | | | 126.5 s |
| 3” | 6.13 (1H, m) | 6.59 | 0.46 | 143.3 d |
| 4” | 1.97 (3H, d, 8.0) | 2.40 | 0.43 | 16.3 q |
| 5” | 1.89 s | 1.89 | 0 | 20.5 q |

Largest deviation $\Delta\delta$ = 1.51 ppm. [a] In 400. [b] In 100 MHz. [c] $\boldsymbol{\Delta\delta}$ = |$\delta$calcd - $\delta$exptl|.

**Scheme S1** Fragment ions of compound **3** in EI spectrum